Controlling the Morphology Evolution of a Particle-Stabilized Binary-Component System

ChemComm

COMMUNICATION

Controlling the Morphology Evolution of a Particle-Stabilized Binary-Component System†

Received 00th January 20xx,
Accepted 00th January 20xx

DOI: 10.1039/x0xx00000x

www.rsc.org/

Tao Li,*[ab] Jason Klebes,[c] Jure Dobnikar,*[ad] and Paul S. Clegg[b]

This work reveals the association of morphology evolution in particle-stabilized binary-component systems (i.e., binary liquids & polymer blends). It investigates the formaion mechanism of bijels created *via* direct mixing, and proposes an empirical cost function to quantitatively evaluate the created structures.

Particle-stabilized binary-component systems can form various morphologies, which often exhibit novel properties and lead to numerous applications.[1] For binary liquids, the composite systems would have dramatic static and dynamic properties, which are wholly different to those of their separate constituents.[2] Polymer blends exhibit a combination of properties that no single commercially available polymer can achieve alone.[3] Besides the conventional Pickering emulsions,[4] multiple emulsions[5], high internal phase emulsions[6] and non-spherical droplets,[7] the jamming of interfacial particles provides a promising route to create even more elaborate arrested states. One remarkable structure, for instance, is known as "bicontinuous interfacially jammed emulsion gel" (bijel), which is a particle-stabilized emulsion with two inter-penetrating continuous phases.[2,8]

By taking advantages of phase inversion, particle stabilized bicontinuity can be produced simply by melt mixing bulk polymers.[9] However, for low molecular-weight liquids, bijels were mainly created by making use of fluid–fluid demixing *via* spinodal decomposition, which demands rapid quenching out of the mixed state of the pair of liquids.[2] This distinction directly indicates the remarkable difference of phase transition behaviors in these two systems, and reveals the importance of viscosity in determining morphologies. The interfacial tension of partially miscible liquids is similar to that of polymer blends (~1 mN/m), but their viscosity can differ by several orders of magnitude.[2,10] Generally, if the proportions of the two components are equal then the lower viscosity component will tend to become the continuous phase so as to reduce dissipation.[11] This also means that the composition at which phase inversion occurs can be tuned by varying the viscosities of the components.[11] Furthermore, increasing the viscosity can slow down the dynamics of the system, which enhances the likelihood of it becoming stabilized in various metastable structures. Very recently, using high viscosity liquids, nanoparticles and a surfactant, we successfully developed a bijel *via* direct mixing at room temperature, which bridges the gap between conventional bijel creation and that of bicontinuous structures using bulk polymers.[12] However, the formation mechanism for bijels created *via* direct mixing is not yet fully understood. Meanwhile, the association of morphology evolution (rather than a certain morphology) in binary liquids and that in bulk polymers is still unclear.

To address these issues, herein, we carry out confocal microscopy studies on mixtures of immiscible glycerol and silicone oil phases; silica nanoparticles and CTAB molecular surfactant are used to stabilize the liquid-liquid interfaces (see the experimental section in ESI†). By adjusting the viscosity ratio of the systems, phase inversion from silicone oil droplets to glycerol droplets is frustrated. The system frustrates inversion which then leads to the preferential formation of bijel-like structures. For the first time, we calculate an empirical cost function to quantitatively evaluate the formed structures, and discussed the phase behaviors with capillary number. The final structures of the system is proved to be a consequence of both break up during mixing and coalescence after mixing. The mechanisms uncovered in this work pave the way for accurately controlling the structures in different particle-stabilized systems, and expand their applications in food, personal care products and new multifunctional soft materials.

In this paper, silicone oils of different viscosity (50 cSt, 1000 cSt and 10000 cSt) were mixed at varying mass fraction as the silicone oil phase. The viscosity ratio of the system (λ_o) is defined as:

$$\lambda_o = \frac{viscosity\ of\ silicone\ oil\ mixture}{viscosity\ of\ glycerol}$$

[a] Beijing National Laboratory for Condensed Matter Physics and Key Laboratory of Soft Matter Physics, Institute of Physics, Chinese Academy of Sciences, Beijing 100190, China. Email: litao444@iphy.ac.cn; jd489@cam.ac.uk
[b] School of Physics and Astronomy, University of Edinburgh, James Clerk Maxwell Building, Peter Guthrie Tait Road, Edinburgh, EH9 3FD, United Kingdom.
[c] School of Mathematics, University of Leeds, LS2 9JT, United Kingdom.
[d] Songshan Lake Materials Laboratory, Dongguan, Guangdong 523808, China.
† Electronic supplementary information (ESI) available: the experimental section.

Fig. 1a, b show the behaviour for high λ_o values. It is clear that particle-stabilized silicone oil droplets (black) have formed within the less viscous glycerol phase (red). The typical droplet diameters are in the 10-20 µm range. It was anticipated that this arrangement would be reversed as the value of λ_o is decreased; however, that is not observed (Fig. 1c-e). As the silicone oil is made progressively less viscous, the preparation protocol results in extended, non-spherical domains of both fluid phases. Again, a very high proportion of the particles (green) are found at the boundaries between the two fluid phases. None-the-less, neither phase has broken up into spherical droplets. So, in spite of having changed the relative viscosity of the two fluid phases, an inversion from silicone oil droplets to glycerol droplets cannot be realized. Interestingly, the frustrated inversion at intermediate λ_o values leads to the preferential formation of bijel-like structures (Fig. 1c, d).

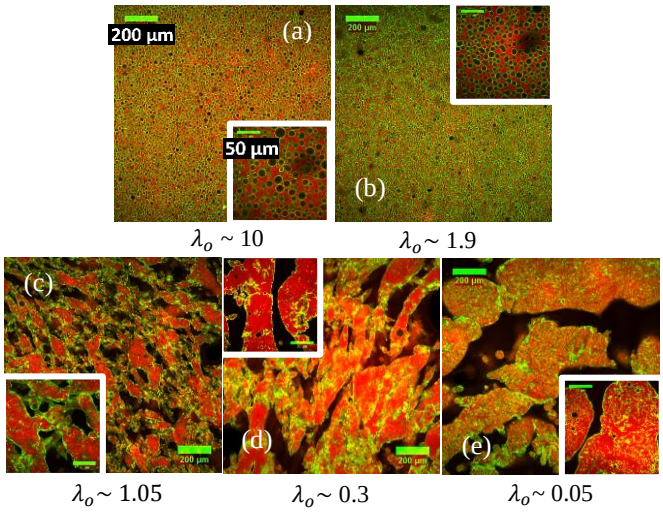

Fig. 1 Confocal micrographs showing the morphology of the domains formed between glycerol and silicone oil as the viscosity ratio (λ_o) is modified. All samples contain ~20 mg of silica particles (green), ~1 mg of CTAB, 1.5g of glycerol (red), and 1.5g of silicone oil phase (black). Shear rate = 3000 rpm (~5,100 s-1). Insets are confocal images at a higher resolution.

Further experiments demonstrated that the morphology changes from roughly spherical droplets to these bijel-like structures over a narrow range in λ_o. Fig. 2a, b and 2c, d show pairs of samples created with very similar λ_o values. The silicone oil for the first pair of images was made up from 10,000 cSt and 50 cSt components (ESI†); the values of λ_o are 1.65 for Fig. 2a, and 1.17 for Fig. 2b, respectively. It can be seen that the slight disparity in λ_o connects the separated silicone oil droplets into extended domains, which eventually makes the silicone oil phase continuous. Similar transition can also be observed when using 1,000 cSt silicone oil instead of 10,000 cSt, as shown in Fig. 2c and d. These observations indicated a critical value of λ_o for this phase transition, which should be situated between 1.19 and 1.65. They also suggest that the absence of an inversion is not a consequence of unexpected chemical changes which occur alongside the variation in the viscosity.

To quantitatively evaluate the obtained bicontinuous structures, an empirical cost function based on the two-dimensional (2D) confocal micrographs has been calculated.[13] The cost function is a composite parameter which characterizes the "bijel-ness" of a sample as observed in a confocal micrograph (i.e. how close a given structure is to a bijel). The crucial features of a 2D image of a bijel are that the two fluid domains have roughly similar areas, the domains are characterized by a typical interface separation which is roughly constant for a given concentration of particles and finally the domains are tortuous i.e. they are not made up of a series of straight channels. Here, we first carry out quantitative image analysis on a binary image after the application of a threshold. The analysis is then repeated on the inverted binary image as both liquid domains should play an identical role in the bicontinuous structure.[13]

In a 2D image of area A, we identify the two phases with areas A_1 and A_2, and the corresponding area fractions $\eta_1 = A_1/A$, $\eta_2 = A_2/A$. It should be noted that, since only areas above a cut-off size can be identified as belonging to the domains, some very small isolated pixels are not counted as a part of the area. Therefore, A1 + A2 ≠ A, and thus $\eta_1 + \eta_2 \neq 1$. We average the area fraction of each phase over all images and obtain the average $< \eta >$, as well as the deviation from the optimal bijel value $\eta_B = 0.5$ (ESI†): $\delta_\eta = (< \eta > - \eta_B)^2 / < \eta >^2$. Another quantifier we evaluate is the domain solidity: $s = A_{domain}/A_{ch}$, where A_{ch} is the area of the convex hull of a domain. The expected bijel value is s_B~ 0.7 (ESI†). Similar to the above, we define the deviation from it: $\delta_s = (< s > - s_B)^2 / < s >^2$. Finally, we also analyze the diameter of the maximum inscribed circle, $\langle \rho \rangle$, quantifying the typical lengthscale in the image, i.e., the average separation between the interfaces. The value typical for bijels is $\rho_B = 23$ µm (ESI†) and the third structure quantifier is thus defined as a deviation from it: $\delta_\rho = (< \rho > - \rho_B)^2 / < \rho >^2$. In order to improve reliability, we evaluate all three quantifiers for both, the direct and the inverted image. In this way, we finally arrive at the expression for the cost function measuring "the bijel-ness" of a given structure:

$$\text{Cost Function} = 1/2\left(\left[\delta_\eta + \delta_s + \delta_\rho\right]_{direct} + \left[\delta_\eta + \delta_s + \delta_\rho\right]_{inverted} \right)$$

The value of the cost function decreases as samples become more bijel-like. Generally, when it is lower than 0.1, the sample is believed to be a bijel. We have evaluated the cost function values for every sample studied and for every λ_o. The results are presented in Fig. 2e, where the data in brackets represent λ_o and the averaged value of its cost function. There is a clear range of viscosity ratios optimal for bijel formation (marked in green). At λ_o = 1.17, the calculated cost function is as low as ~19.8×10^{-3}, indicating two uniform, interpenetrating and continuous liquid phases (see Fig. 2b). Increasing or decreasing λ_o leads to significant increase of the cost function value, which raises to higher than 400 for the silicone oil droplets when λ_o > 1.6, and around 200 for large distorted doamins when λ_o < 0.1.

The calculated cost function and the observed structures are helpful to better understand the formation mechanisms of different morphologies in a binary-component system, especially for the creation of bijels *via* direct mixing. It was believed that the dynamics of droplets under shear can be determined by the ratio between the viscous deformation stresses (shear stress) and the restoring

interfacial stresses (Laplace pressure),[14] given by the capillary number:

$$C_a = \frac{shear\ stress}{Laplace\ pressure} = \frac{\lambda \dot{\gamma} R_0}{\sigma} \quad (1)$$

where $\dot{\gamma}$ is the shear rate, R_0 is the radius of the spherical domain, σ is the interfacial tension, and notably, λ is the viscosity of the continuous matrix. Once the value of C_a exceeds a critical threshold, large droplets would deform and eventually break up under the influence of shear.[15] In our experiments, $\dot{\gamma}$ (~ 5100^{-1}) and σ (~ 21.2 ± 0.5 mN/m) were both kept constant; low and high frequency rheology show that the measured viscosity values change little between 10 s^{-1} and 5000 s^{-1}, indicating no significant shear thinning or thickening for all systems (Fig. 3a, also see the experimental section in ESI†). When the viscosity of the silicone oil mixture is larger than that of the glycerol phase (i.e., λ_o > 1), glycerol would tend to be continuous under shear as the less viscous liquid. As a result, small silicone oil droplets were created and separated in glycerol as illustrated in Fig 1a and b. In this case, the value of C_a keeps constant, which explains why the size of the silicone oil droplets barely changes with a significant reduction in λ_o from 10 (Fig. 1a) to ~1.9 (Fig. 1b).

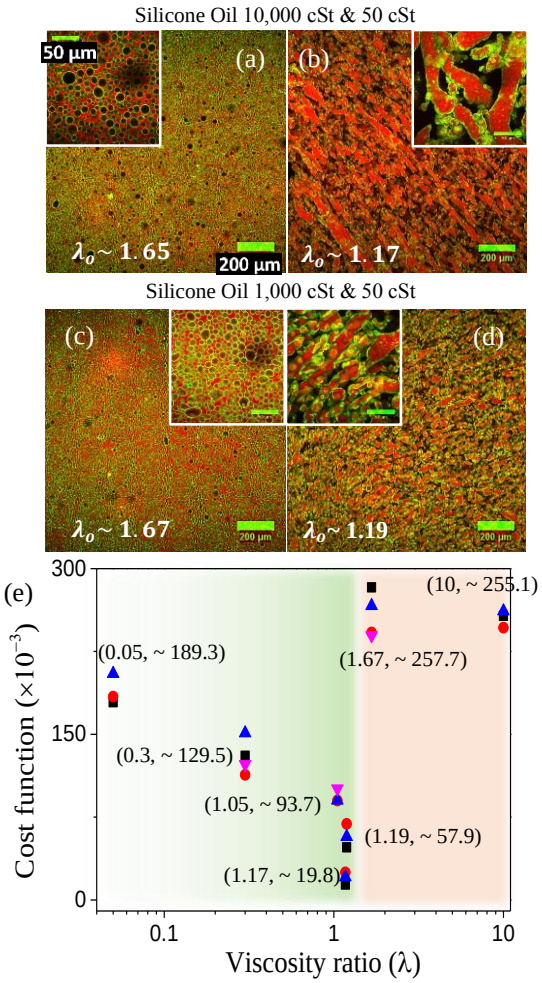

Fig. 2 (a-d) The created structures of samples with very similar λ_o values but different chemical components. The silicone oil was made up from 10,000 cSt & 50 cSt components for (a, b), and 1,000 cSt & 50 cSt components for (c, d). Shear rate = ~5,100 s^{-1}. (e) The calculated cost function for different λ_o . Each λ_o has multiple calculated cost function values (the dots marked in different colors); data in brackets represent λ_o and its averaged cost function.

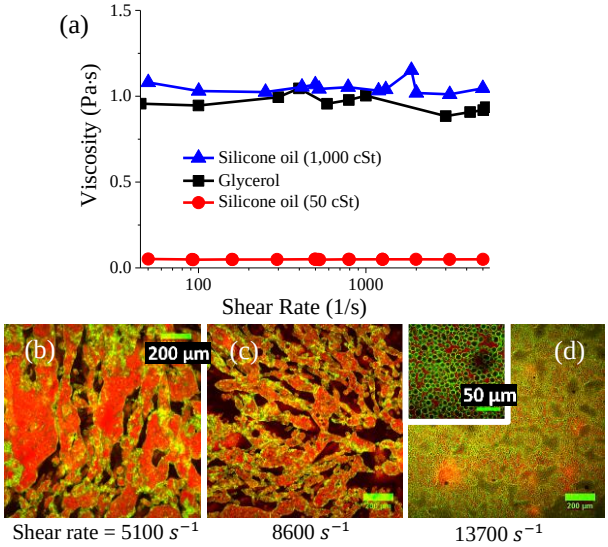

Fig. 3 (a) Viscosity as a function of shear rate of glycerol (black) and silicone oils (50 cSt, red; 1000 cSt, blue). (b-d) The morphologies obtained by mixing the same system (λ_o = 0.3) at different shear rate.

When λ_o is much lower than 1, as shown in Fig. 1d and e, silicone oil became the continuous phase; large and distorted domains of glycerol were created after shearing the systems. Remarkably, there were still nanoparticles dispersing inside the glycerol phase instead of being trapped at the interface. It is known that the structures can only be stabilized once the interfaces have been fully coated with particles; before that, domains from the same component would coalesce. The coalescence process makes the dynamics of the liquid domains more complex, and results in anisotropic structures. This opens up the way for controllable morphology evolution in our systems, which can be achieved by varying the shear rate (i.e., the $\dot{\gamma}$ in Eq. 1). In Fig. 3b-d, , we present results for samples formed at the same λ_o value (~ 0.3, identical to that for Fig. 1d) but at the shear rates (b) 5,100 s^{-1} (c) 8,600 s^{-1} (d) 13,700 s^{-1} respectively. From Eq. (1), the interface separation should decrease in proportion to the increase in the shear rate, i.e., by a factor of approximately three across this range of samples. Instead we observe a decrease of significantly more than an order of magnitude across this range. Meanwhile, the amount of interface coated with particles in Fig. 3d is vastly higher than that in Fig. 3b. These results not only prove that the shear rate can influence the size of the domains that the samples are broken up into, but also suggest that besides Ca, the coalescence plays an important role in structure formation. The final structure of the system should be a consequence of both break up during mixing and coalescence after mixing (see the shear time effect, Fig. S1, ESI†).

For a system where the viscosity of the silicone oil mixture is roughly equal to that of the glycerol phase, i.e., λ_o ~1, a balance between the break up and the coalescence can be achieved when shearing at an appropriate rate. Since there is no less-viscous liquid, both liquids would tend to be continuous. The high viscosity of the liquids

increases the likelihood of small domains coalesce into cross-linked structures and slows down their relaxation. At the same time, nanoparticles are trapped onto the newly created interfaces, locking the formed structures in a three-dimensional (3D) space.16 This can be one of the formation mechanisms for the bijels observed in Fig. 1c, 2b, d and 3c.

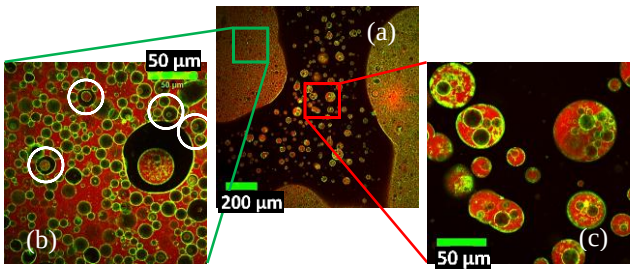

Fig. 4 (a) Two different types of multiple emulsions created by shearing a high-viscosity system (λ_o = 1.9) at a low rate (1,700 s^{-1}). (b) Glycerol-in-silicone oil-in-glycerol multiple droplets (marked by white circles). (c) Silicone oil-in-glycerol-in-silicone oil multiple droplets.

We have shown that, by varying λ_o and $\dot{\gamma}$, large glycerol domains, bijels and small silicone oil droplets can all be created in a particle-stabilized binary-fluid system. Beyond these structures, emulsions comprised of glycerol droplets can also been yielded when shearing an intermediate viscos system at a low rate (Fig. 4a, λ_o ~ 1.6, $\dot{\gamma}$ ~ 1,700 s^{-1}). However, these droplets are found in the context of complex multiple emulsion domains. In the glycerol-rich phase, some glycerol-in-silicone oil-in-glycerol (G/S/G) multiple droplets can be observed (marked white in Fig. 4b). Meanwhile, in the silicone oil-rich phase, the opposite situation, silicone oil-in-glycerol-in-silicone oil (S/G/S) multiple droplets, was observed (Fig. 4c). This coexistence of two different types of multiple emulsions has not been reported previously. It should be pointed out that multiple emulsion droplets with the hierarchy S/G/S are not stable. They coalesce with neighbours forming larger droplets, some of which are non-spherical (Fig. 4c). By contrast, G/S/G multiple emulsions are highly stable. Upon shearing at a higher shear rate the entire system becomes an emulsion of silicone oil droplets. These results demonstrate that, to some limited extent, inversion to the formation of particle-stabilized glycerol droplets is possible but it only occurs in the context of highly heterogeneous samples. The composites clearly have a very marked resistance to forming simple emulsions comprised of particle-stabilized glycerol droplets alone.

We believe this resistance is caused by the hydrophilic property of the used particles, which makes them preferentially wetted by glycerol and thus frustrates the phase inversion to glycerol droplets.[17] This can be critical for understanding and controlling the formation of bijels by mixing, since the inversion-frustrated system leads to the preferential formation of bicontinuous structures (Fig. 1). Previously, using bulk polymers, similar bicontinuity has been achieved *via* direct mixing.[9a] It is worth nothing that, unlike this study, the polymer blends need to be sheared at a melt temperature, and no multiple emulsions can be created.

In conclusion, this study reveals the formation mechanisms for bijels created *via* direct mixing, and fills an important gap between the morphology evolution in low molecular weight liquids (e.g. water & 2,6-lutidine)[2] and that in bulk polymers. For the first time, an empirical cost function is applied to quantitatively evaluate the observed structures, which provides a new tool for theoretical studies in emulsion science. The final structure of the system is a consequence of both break-up during mixing and coalescence after mixing, which can be governed by varying the viscosity ratio and the shear rate. The mechanisms uncovered in this work make it possible to use one phenomenon to push the system towards the inversion, while another is deployed to prevent the process going to completion; different morphologies can be created and transformed into each other in the same system. This greatly expands the versatility of particle-stabilized binary-component systems, and can be used to design novel multifunctional soft materials.

Conflicts of interest

There are no conflicts to declare.

Notes and references

1 (a) P. S. Clegg, *J. Phys.: Condens. Matter*, **2008**, *20*, 113101. (b) M. N. Lee, A. Mohraz, *J. Am. Chem. Soc.*, **2011**, *133*, 6945–6947. (c) S. T. Krishnaji, W. W. Huang, O. Rabotyagova, E. Kharlampieva, I. Choi, V. V. Tsukruk, R. Naik, P. Cebe, D. L. Kaplan, *Langmuir*, **2011**, *27*, 1000–1008.
2 E. M. Herzig, K. A. White, A. B. Schofield, W. C. K. Poon, P. S. Clegg, *Nat. Mater.*, **2007**, *6*, 966–971.
3 (a) N. D. B. Lazo, C. E. Scott, *Polymer*, **2001**, *42*, 4219–4231. (b) D. R. Paul, J. W. Barlow, *J. Macromol. Sci-Rev. Macromol. Chem.*, **1980**, *C18*, 109–168.
4 (a) S. U. Pickering, *J. Chem. Soc.*, **1907**, *91*, 2001–2021. (b) W. Ramsden, *Proc. R. Soc. London*, **1903**, *72*, 156–164.
5 P. S. Clegg, J. W. Tavacoli, P. J. Wilde, *Soft matter*, **2016**, *12*, 998–1008.
6 (a) T. Zhang, Y. Wu, Z. Xu, Q. Guo, *Chem. Commun.*, **2014**, *50*, 13821-13824. (b) D. Cai, J. H.T. Thijssen, P. S. Clegg, *ACS Appl. Mater. Interfaces*, **2014**, 6, 9214-9219.
7 (a) C. Mengmeng, T. Emrick, T. P. Russell, *Science*, **2013**, *342*, 460–463. (b) L. Becu, L. Benyahia, *Langmuir*, **2009**, *25*, 6678–6682.
8 K. Stratford, R. Adhikari, I. Pagonabarraga, J.-C. Desplat, M. E. Cates, *Science*, **2005**, *309*, 2198–2201.
9 (a) M. Si, T. Araki, H. Ade, A. L. D. Kilcoyne, R. Fisher, J. C. Sokolov, M. H. Rafailovich, *Macromolecules*, **2006**, *39*, 4793–4801. (b) P. Potschke, D. R. Paul, *J. Macromol. Sci., Polym. Rev.*, **2003**, *C43*, 87–141.
10 H-j. Chung, K. Ohno, T. Fukuda, R. J. Composto, *Macromolecules*, **2007**, *40*, 384–388.
11 B. P. Binks, A. T. Tyowua, *Soft matter*, **2016**, *12*, 876–887.
12 D. Cai, P. S. Clegg, T. Li, K. A. Rumble, J. W. Tavacoli, *Soft matter*, **2017**, *13*, 4824–4829.
13 W. Rasband, ImageJ 1.50i, http://imagej.nih.gov/ij/.
14 Y. Mei, G. Li, P. Moldenaers, R. Cardinaels, *Soft Matter*, **2016**, *12*, 9407–9412.
15 H. P. Grace, *Chem. Eng. Commun.*, **1982**, *14*, 225–277.
16 J. Giermanska-Kahn, V. Laine, S. Arditty, V. Schmitt, F. LealCalderon, *Langmuir*, **2005**, *21*, 4316–4323.
17 D. Cai, P. S. Clegg, *Chem. Commun.*, **2015**, *51*, 16984–16987.